

# Learning to Project for Cross-Task Knowledge Distillation

Dylan Auty\*, Roy Miles\*, Benedikt Kolbeinsson\*, and Krystian Mikolajczyk

Imperial College London

**Abstract.** Traditional knowledge distillation (KD) relies on a proficient teacher trained on the target task, which is not always available. In this setting, cross-task distillation can be used, enabling the use of any teacher model trained on a different task. However, many KD methods prove ineffective when applied to this cross-task setting. To address this limitation, we propose a simple modification: the use of an inverted projection. We show that this drop-in replacement for a standard projector is effective by learning to disregard any task-specific features which might degrade the student’s performance. We find that this simple modification is sufficient for extending many KD methods to the cross-task setting, where the teacher and student tasks can be very different. In doing so, we obtain up to a 1.9% improvement in the cross-task setting compared to the traditional projection, at no additional cost. Our method can obtain significant performance improvements (up to 7%) when using even a randomly-initialised teacher on various tasks such as depth estimation, image translation, and semantic segmentation, despite the lack of any learned knowledge to transfer. To provide conceptual and analytical insights into this result, we show that using an inverted projection allows the distillation loss to be decomposed into a knowledge transfer and a spectral regularisation component. Through this analysis we are additionally able to propose a novel regularisation loss that allows teacher-free distillation, enabling performance improvements of up to 8.57% on ImageNet with no additional training costs.

## 1 Introduction

Knowledge distillation (KD) has emerged as a very effective tool for training small and efficient models [5, 21, 44, 49, 52, 70]. It leverages the pre-trained knowledge of a much larger (teacher) model to guide and enhance the training process of a significantly smaller (student) model. Since its inception, KD has been applied to a wide variety of tasks in the computer vision [10], audio [14] and language [64] domains, enabling the deployment of models across many embedded devices.

However, existing approaches for KD are often limited to the cases where the teacher shares the same task with the student [9–11, 29, 31, 70]. This is

---

\* These authors contributed equally.

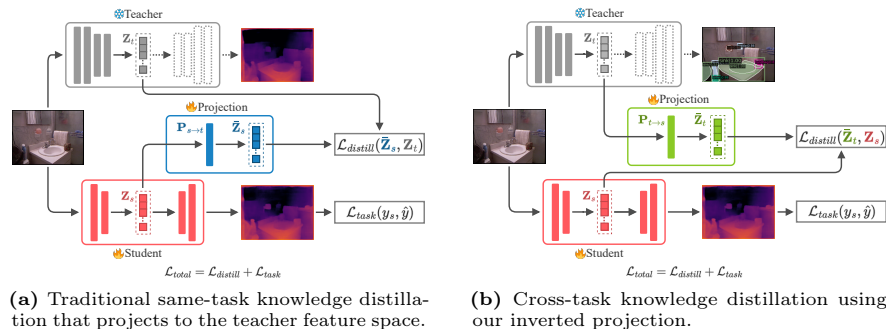


**Fig. 1: Our cross-task knowledge distillation pipeline**, where a student model is trained on a target task with the aid of a frozen teacher that is pretrained on a **different** task. Compared to standard same-task feature distillation (fig. 1a), our cross-task approach uses an *inverted projector* (fig. 1b) which is able to discard irrelevant task-specific features from the different-task teacher. The loss comprises a feature distillation loss  $\mathcal{L}_{distill}$  that matches the student features with the projected teacher features, and a task-specific supervised loss  $\mathcal{L}_{task}$  applied only to the student model’s output for the target task.  $\text{🔥}$  denotes trainable weights, while  $\text{🌟}$  denotes weights that are frozen throughout training.

very restrictive since there are many applications where there is simply no suitable pretrained teacher available due to, for example, the lack of any large annotated training data. This problem commonly arises for tasks that require expensive human annotation [46], such as in robotics [33], or where the collection of data is prohibitive for other reasons, such as in the medical [38, 63] and aerial domains [23, 36, 74]. In these cases, it is not possible to train a suitable teacher for the target task, therefore we propose a **cross-task knowledge distillation**. In the cross-task KD setup, a teacher model trained for a **different** task can be used to improve the student performance. This setting is well-suited for tasks lacking a task-specific pretrained teacher, as it allows for any other off-the-shelf pretrained model to be used to improve the student model performance instead. It is also increasingly relevant as the compute and data costs to train large models increases. Similarly, data labelling may be cheaper for one task than another, e.g. training a model using a cheaply-labelled auxiliary task is very common in active learning [4, 25, 30] and federated learning [1].

We show that the traditional methods for same-task KD fail in this new and more general cross-task setting since they transfer domain-specific knowledge, which is associated with the *teacher’s* task. Therefore, while they increase the student’s performance in the traditional same-task setting, they degrade it in the cross-task scenario. We propose the use of an inverted projection to address this problem. We find that this modification is very effective in the cross-task setting due to its suppression of task-specific information. Most notably, we can obtain up to a 7.47% performance improvement by distilling from a teacher trained on various different tasks. We demonstrate that this simple drop-in

replacement enables many KD methods to adapt to the cross-task setting, and we show consistent improvements across various tasks including depth estimation, segmentation, and image translation.

To obtain more insights into the underlying mechanism of the inverted projector, we explore the training dynamics of its weights. We find that the least-significant singular vectors of the teacher’s features are suppressed in cases where there is a significant task gap, which indicates that these singular vectors tend to be more task-specific. Based on this observation we show that the suppression of singular vectors by the projector naturally leads to a decoupling of the distillation loss into a knowledge transfer and spectral regularisation component. This enables us to derive a **cheap spectral regularisation loss**. We describe this loss as a *teacher-free distillation* method since it explicitly exploits the emergent regularisation component from cross-task distillation. The new loss makes it possible to efficiently achieve performance competitive with many state-of-the-art KD methods without the need for any pre-trained teachers, with a 3.2% relative improvement over the baseline model on ImageNet-1K. In summary, our contributions are given as follows:

- We propose a simple modification to standard KD that enables cross-task distillation: a learnable inverted projection.
- We show consistent and substantial performance improvements in the cross-task setting of up to 7% through extensive experiments.
- By analysing the training dynamics of the projector weights, we are able to decouple a knowledge transfer and spectral regularisation component. We use this to derive a teacher-free regularisation loss that obtains up to 8% improvement over the baseline with no additional training cost.

## 2 Related Work

**Knowledge distillation (KD)** is a technique that involves transferring the knowledge from a large teacher model to a smaller student model, aiming to improve the performance of the student on the target task. It has become increasingly popular in recent years for the deployment of models on resource constrained devices, such as mobile phones, and has been applied in image classification [9, 29], semantic segmentation [42], video object segmentation [52], and natural language processing [65]. Existing literature has extensively explored various distillation pipelines [39, 45, 60] along with both empirical and theoretically motivated loss formulations [9, 29, 51, 82] that can facilitate the knowledge transfer process. However, these conventional methods still predominantly focus on same-task distillation [10, 70], wherein the student and teacher models are trained on the same task. There are many applications where there are no pre-trained off-the-shelf teacher models available, thus motivating the need to perform *cross-task distillation*. Some prior works have pursued cross-task distillation both as a generalisation of the knowledge transfer occurring in traditional knowledge distillation [78] and because of the observation that some tasks will naturally

tend to share information [76, 79]. CrossDistil [76] was one of the first to partially explore this new setting by introducing a quadruplet loss, calibration term, and an error correction mechanism, however knowledge was distilled between the task-specific decoder heads of a multi-task model with shared encoder weights, rather than between two fully-separate models. ProC-KD [40] transfer local-level object knowledge for large-scale cross-task distillation, while [78] construct a relational embedding for the loss. [79] perform cross-task KD to augment text-to-image generation using image semantic encoders, but the proposed method is tightly coupled with the model architecture at each stage of the pipeline. In contrast to these works, we propose a very simple extension to the typical feature distillation pipeline that enables the distillation of knowledge cross-task across a wide range of settings.

**Transfer learning and domain adaptation** are widely studied areas in machine learning that leverage the knowledge acquired by a pretrained model on one task to enhance the performance on a different, yet related task [85]. This paradigm has demonstrated significant success in various fields, especially in computer vision [20, 81] and natural language processing [58, 68], by reducing the training time and data requirements in the target domain. Most existing transfer learning or domain adaptation algorithms attempt to align the feature representations across the two domains. This can be achieved by minimising some statistical discrepancy between the two spaces [27] or introducing additional adversarial losses [17]. More recent works [13] have shown a spectral divide between the domain-specific and domain-agnostic features. This is where the large singular values of the features can generalise across domains, whereas the small singular values are domain-specific. This observation has led to follow-up works [12, 13, 55] by proposing spectral alignment and normalisation techniques. We take a similar approach for transferring knowledge between different tasks, but in the context of knowledge distillation, where an additional capacity gap between the source and target task models exists. This work also enables a more concrete bridge between the field of transfer learning and knowledge distillation.

**Multi-task learning.** There are many cases where jointly training on multiple tasks or modalities can improve not only the generality of models [56] but also the single-task performance. For example, monocular depth estimation has been shown to share knowledge with other tasks, such as semantic segmentation [2, 3, 34, 37, 59, 73, 75]. Intuitively, this follows for other task pairs; for instance, both semantic segmentation and classification target the semantics within an image. Unfortunately, multitask models are often too large and expensive to run on resource-constrained devices [35]. Additionally, jointly learning multiple tasks with a small model can degrade the downstream performance, as additional tasks or objectives can conflict with the target task when there is insufficient capacity in the student to optimise for both [22]. This further motivates our approach to training efficient models for a single task by leveraging cross-task information.

### 3 Method

This section describes our proposed inverted projection and our pipeline for cross-task distillation. We first describe the cross-task knowledge distillation setting and detail why the typical approaches for same-task KD which use the traditional projector are not suited to it, particularly when there is a significant difference between the teacher and student tasks. We then present our inverted projection and analyse its dynamics to help understand the underlying principles of cross-task distillation. Finally, we use this analysis to derive a straightforward drop-in *teacher-free* distillation loss that provides some of the benefits of knowledge distillation *without* the use of any teacher model.

#### 3.1 Cross-task Feature Distillation

Cross-task distillation is motivated by the intuitive and demonstrated overlap in useful information between different tasks (see section 2). We use feature-space distillation, which aims to align the feature spaces of a student model and a teacher model. To do this, a learnable projection is used to map the features from one model into the feature space of the other. However, in the cross-task case, where the teacher model has been trained for a significantly different task to the student model’s target task, there are specific issues to contend with that traditional KD methods do not address.

We introduce a novel inverted projection that is well-suited to the cross-task setting, in contrast to the traditional projection [62, 70] which is better suited to the same-task setting. In section 3.2, we provide the motivation for our method, and in section 3.3 we describe our pipeline, problem setup, and loss function.

#### 3.2 Importance of Feature Projection

In the traditional same-task setting, the teacher model is already pre-trained for the student’s target task, so it is desirable for the student to match features as closely as possible with those produced by the teacher. In this case, the task-specific knowledge is helpful in improving the student performance. However, for the cross-task setting, the teacher is trained on a different task to the student. As detailed in section 2, there is likely at least some shared knowledge between different tasks. The issue in the cross-task knowledge distillation setting is how to extract only the *task-agnostic* knowledge and the knowledge *shared* between tasks, all while ignoring the irrelevant features produced by teacher. This last point is especially important for smaller student models as they do not have the capacity to effectively learn the union of two very different feature spaces.

A projection layer is often used in knowledge distillation to match the student’s feature dimensions with those of the teacher [62, 70]. Although recent works have highlighted the importance of the projector in improving the efficacy of same-task distillation [15, 48, 50], they have proven ineffective when there is cross-task information present. We propose a modification of the projection in which we instead map from the teacher space onto the student space. We describe this as

**Table 1: Cross-task distillation to a depth estimation student model using similar (■) and dissimilar (■) teacher tasks**, showing the **increasing** effect of our inverted projection as similarity between teacher and student tasks **decreases**. We use our inverted projector with four different KD methods to show its general applicability. The inverted projector outperforms traditional projections in the cross-task case for which it is designed, but always produces a performance improvement over the baseline (no distillation) regardless of the teacher task. ■ ■ ■ ■ colour map denotes *decreasing* student-teacher task similarity. Results on NYUv2 [66] using an EfficientNet-B0 [69]-based student.

Teacher task →		■ Depth			■ Instance Seg.			■ Classification			■ Random		
KD Method	Projection type	$\delta_1 \uparrow$	Abs. ↓	RMS ↓	$\delta_1 \uparrow$	Abs. ↓	RMS ↓	$\delta_1 \uparrow$	Abs. ↓	RMS ↓	$\delta_1 \uparrow$	Abs. ↓	RMS ↓
<i>No teacher (baseline)</i>		0.845 ±0.007	0.127 ±0.003	0.440 ±0.005	0.845 ±0.007	0.127 ±0.003	0.440 ±0.005	0.845 ±0.007	0.127 ±0.003	0.440 ±0.005	0.845 ±0.007	0.127 ±0.003	0.440 ±0.005
FitNets [62] ICLR 2015	Traditional	<b>0.868</b>	<b>0.117</b>	<b>0.406</b>	<b>0.855</b>	<b>0.122</b>	<b>0.425</b>	0.845	0.125	0.439	0.828	0.134	0.455
	Inverted (ours)	0.849	0.124	0.432	0.851	0.124	0.431	<b>0.850</b>	<b>0.124</b>	<b>0.434</b>	<b>0.851</b>	<b>0.124</b>	<b>0.431</b>
	Improvement	-2.17%	-6.35%	-6.49%	-0.41%	-1.78%	-1.31%	0.50%	0.53%	1.34%	2.86%	7.47%	5.20%
AT [80] ICLR 2017	Traditional	<b>0.856</b>	<b>0.122</b>	0.426	0.852	0.123	0.431	0.850	0.125	0.433	<b>0.857</b>	<b>0.121</b>	<b>0.428</b>
	Inverted (ours)	<b>0.856</b>	<b>0.122</b>	<b>0.425</b>	<b>0.855</b>	<b>0.121</b>	<b>0.429</b>	<b>0.853</b>	<b>0.123</b>	<b>0.430</b>	<b>0.857</b>	0.122	<b>0.428</b>
	Improvement	-0.11%	-0.08%	0.02%	0.42%	1.38%	0.53%	0.35%	1.61%	0.79%	0.05%	-0.83%	0.09%
PKT [54] ECCV 2018	Traditional	<b>0.854</b>	<b>0.122</b>	0.429	<b>0.857</b>	<b>0.123</b>	<b>0.427</b>	0.851	0.124	0.432	0.856	0.123	0.429
	Inverted (ours)	<b>0.854</b>	<b>0.122</b>	<b>0.427</b>	0.854	<b>0.123</b>	0.429	<b>0.853</b>	<b>0.123</b>	<b>0.431</b>	<b>0.858</b>	<b>0.122</b>	<b>0.426</b>
	Improvement	0.04%	-0.16%	0.42%	-0.34%	-0.08%	-0.44%	0.25%	1.29%	0.30%	0.29%	1.22%	0.84%
Ensemble [15] NeurIPS 2022	Traditional	<b>0.861</b>	<b>0.119</b>	<b>0.416</b>	<b>0.856</b>	<b>0.122</b>	<b>0.425</b>	<b>0.852</b>	<b>0.124</b>	<b>0.431</b>	0.835	0.128	0.446
	Inverted (ours)	0.849	0.124	0.433	0.848	0.124	0.435	0.847	0.125	0.437	<b>0.849</b>	<b>0.124</b>	<b>0.432</b>
	Improvement	-1.46%	-4.64%	-4.11%	-0.95%	-1.64%	-2.16%	-0.63%	-0.89%	-1.30%	1.74%	2.75%	3.03%

*inverting* the projector, and we find that it enables the suppression of irrelevant (task-specific) features. We show that this inverted projector can effectively discard these irrelevant features if needed. If this were to be used in the traditional same-task setting, the discarding of these features would be detrimental, but in the cross-task setting, it is actively desirable.

### 3.3 Setup and Training loss

Our cross-task knowledge distillation pipeline is shown in figure 1b. It consists of a trainable student model, which is to be trained on a given target task, and a frozen teacher model, which is pre-trained on a different task. This setup is in contrast to the traditional same-task knowledge distillation setting, which is shown in figure 1a. Both the student and teacher models receive the same input image, and their respective encoders produce features  $\mathbf{Z}_s$  and  $\mathbf{Z}_t$  respectively. A learnable linear projection matrix  $\mathbf{P}$  is used to project  $\mathbf{Z}_t$  to the dimensions of  $\mathbf{Z}_s$ , giving  $\tilde{\mathbf{Z}}_t = \mathbf{Z}_t \mathbf{P}$ . A distance function  $d$  is then used between the student features and the projected teacher features:

$$\mathcal{L}_{distill} = d(\mathbf{Z}_s, \mathbf{Z}_t \mathbf{P}), \quad (1)$$

where  $d$  can be any distance metric, such as the L2 loss used by FitNets [62] or the attention mapping described by AT [39]. In addition to this loss, we also use a task-specific supervision loss between the student model’s output  $y_s$  and the ground truth labels  $y$  to ensure the student’s output aligns with the target task.

Since the teacher’s output is not used, we only perform a forward pass through its encoder in order to reduce the training compute required. The final loss is given by:

$$\mathcal{L}_{total} = \mathcal{L}_{task}(y_s, y) + \mathcal{L}_{distill}(\bar{\mathbf{Z}}_t, \mathbf{Z}_s), \quad (2)$$

where  $\mathcal{L}_{task}$  is the downstream target-task loss. For example, for depth estimation it will be a pixel-wise loss with the ground truth depth, and for image classification it will be a cross entropy term.

### 3.4 Decoupled Feature Distillation

To obtain analytical insights into the consequences of projecting the teacher features, we take the case where  $\mathcal{L}_{distill}$  is a simple L2 loss between the student’s features  $\mathbf{Z}_s$  and the projected teacher features  $\bar{\mathbf{Z}}_t$ . We perform singular value decomposition on both, i.e.  $\bar{\mathbf{Z}}_t = \bar{\mathbf{U}}\bar{\Sigma}\bar{\mathbf{V}}^T$  and  $\mathbf{Z}_s = \mathbf{U}\Sigma\mathbf{V}^T$ . The cross-task setting requires that our inverted projection learns to discard the irrelevant task-specific features from the teacher model. This can be implemented using a low-rank projection of the features. However, we observe that a low-rank projection naturally emerges in the cross-task setting when using our inverted projector. In fact, this emergence is even more prominent when there is a significant task gap (see section 4). Using this low-rank property, we can express  $\bar{\mathbf{Z}}_t$  using a truncated SVD, i.e. keeping few non-zero singular values. Substituting this into our  $\mathcal{L}_{distill}$  with an L2 loss, we can then decouple an upper bound into a knowledge transfer and a spectral regularisation component<sup>1</sup>:

$$\mathcal{L}_{distill} = d(\mathbf{Z}_s, \mathbf{Z}_t\mathbf{P}) \rightarrow \|\mathbf{Z}_s - \mathbf{Z}_t\mathbf{P}\|_2 \quad \text{e.g. FitNet loss} \quad (3)$$

$$= \left\| \sum_{i \in k} (\bar{\sigma}_i \bar{\mathbf{u}}_i \bar{\mathbf{v}}_i^T - \sigma_i \mathbf{u}_i \mathbf{v}_i^T) + \sum_{i \notin k} \sigma_i \mathbf{u}_i \mathbf{v}_i^T \right\|_2 \quad \text{Low-rank projection} \quad (4)$$

$$\leq \underbrace{\left\| \sum_{i \in k} \bar{\sigma}_i \bar{\mathbf{u}}_i \bar{\mathbf{v}}_i^T - \sigma_i \mathbf{u}_i \mathbf{v}_i^T \right\|_2}_{\text{knowledge transfer}} + \underbrace{\left\| \sum_{i \notin k} \sigma_i \mathbf{u}_i \mathbf{v}_i^T \right\|_2}_{\text{regularisation}}, \quad \text{Decoupled upper bound} \quad (5)$$

where  $k$  denotes the set of indices indexing the non-zero singular values of  $\bar{\mathbf{Z}}_t$ . In practice, any metric  $d$  that satisfies the triangle inequality has this decoupled upper bound in the cross-task setting. This result shows that the distillation loss can be decomposed into a knowledge transfer and an implicit spectral regularisation component. It explains how the inverted projection can help to improve performance even when there is little or no knowledge to transfer from the teacher: through a low-rank regularisation on the feature space.

### 3.5 Teacher-Free Distillation

The decoupled feature distillation in equation 5 allows us to introduce a novel spectral regularisation loss  $\mathcal{L}_{spectral}$ . This loss captures the regularisation effect

<sup>1</sup> For full details, please see the supplementary material.



of the cross-task distillation process without the use of any teacher, therefore we call this method "*teacher-free distillation*". It minimises the least-significant singular vectors of the student model's features while keeping the most-significant. We define the spectral regularisation loss as follows. Assuming that the singular values/vectors are sorted from most to least significant, the loss can be given as follows:

$$\mathcal{L}_{spectral} = \left\| \sum_{i=r}^{rank} \sigma_i \mathbf{u}_i \mathbf{v}_i^T \right\|_2, \quad (6)$$

where  $r$  is a hyperparameter expressing the strength of the regularisation loss and  $rank$  is the rank of the student features. More concretely, this hyperparameter defines the number of singular values being preserved. A smaller  $r$  will result in more singular values being suppressed, thus leading to a more aggressive regularisation of the feature space. In general, this loss effectively penalises the reconstruction of features by the least significant singular values. It suppresses the features that are overly task-specific, thus forcing the representation into a lower rank space, which leads to better generalisation. We perform experiments using this loss in section 4.6.

## 4 Experiments and Results

To validate the efficacy of our inverted projector in the cross-task setting, we perform experiments ablating across different distillation methods, task pairs, and architectures. We experiment with four target tasks: monocular depth estimation, semantic segmentation, image colourisation, and satellite-to-map translation. For each of these student tasks, teacher tasks are chosen that are either identical, similar, or different to them, thus demonstrating that our method is best-suited for the cross-task case where there are significant differences in the task specific knowledge learned by the teacher and student models.

**Randomly-initialised teachers.** An interesting question arises when we consider increasingly disparate student and teacher tasks: what happens if a *randomly-initialised* teacher is used? In this case, there is no knowledge shared between the teacher's task and the target task, however the random weights in the teacher may still produce diverse features. To investigate this question, we also distill from randomly initialised teacher models in our experiments.

In the following sections, we first give the implementation details and then present the results for the specific student tasks. In all of these setups, the teacher model is frozen, and the inverted projection and student model are jointly trained end-to-end using the loss function shown in equation 2.

### 4.1 Implementation details

The general framework used is described in section 3, and shown in figure 1b. The model architectures used for the student and teacher vary depending on the task pairs. As an example, our depth estimation student is an encoder-decoder architecture with either a MobileNetV2, ResNet50, or EfficientNet-B0 backbone,



**Table 2: Comparison for different cross-task settings.** We observe that our inverted projector is effective across many different task pairs and even for the same-task distillation settings.

(a) Semantic segmentation			(b) Colourisation			(c) Satellite-to-map conversion		
Teacher Task	IoU $\uparrow$	Pix. Acc. $\uparrow$	Teacher Task	PSNR $\uparrow$	FID $\downarrow$	Teacher Task	PSNR $\uparrow$	FID $\downarrow$
<i>No teacher</i>	34.60 $\pm 0.36$	0.759 $\pm 0.001$	<i>No teacher</i>	20.48 $\pm 0.04$	65.77 $\pm 1.21$	<i>No teacher</i>	35.29 $\pm 0.18$	67.43 $\pm 1.70$
Random	<b>37.20</b>	<b>0.768</b>	Random	20.99	63.23	Random	35.28	72.54
Classif.	36.00	0.766	Seg.	21.10	63.44	Classif	<b>36.29</b>	<b>59.86</b>
Seg.	36.50	0.767	Classif	<b>21.27</b>	65.92			
			Depth	20.84	<b>62.60</b>			

and the frozen teacher model is a ViT-B/32 [18] trained for classification or the SwinV2-B [43] backbone of AiT [53] pretrained for instance segmentation. All architectures used follow an encoder-decoder structure. The student and teacher features,  $\mathbf{Z}_s$  and  $\mathbf{Z}_t$ , are extracted immediately after the encoder of the model in question. All decoders used require features with a spatial (height and width) dimension, therefore if the teacher model’s encoder has a final pooling layer (as in the case of the classification teacher), this is removed. Full architectural details for the models used for each task pair are included in the supplementary material.

## 4.2 Monocular depth estimation

Monocular depth estimation is the task of inferring the depth, or distance to the camera, of every point shown in a single image. It is a challenging problem, as there is a many-to-one mapping from 3D scenes to a given 2D depth-image, but nonetheless deep learning methods have been able to perform very well by learning suitable priors over the data.

When experimenting with depth estimation as a target task, we make use of teachers trained on tasks that range from similar to dissimilar to the target task of depth estimation, in terms of the overlap in knowledge. We use a depth teacher for the same-task distillation, and the instance segmentation and classification tasks for the increasingly dissimilar teacher tasks. Finally, we use a randomly initialised and frozen teacher for the most extreme cross-task setting. Experiments are run on the NYUv2 dataset [66].

Our results are shown in table 1. As expected (see section 3), the use of our inverted projection produces improvements in performance when using *dissimilar* teacher tasks (random and classification), and gives similar or worse performance when the teacher’s task is similar to the target (instance segmentation and depth estimation teachers).

We use four different feature distillation methods from the same-task literature to show the utility of our method as a drop-in for use in the cross-task setting: FitNets [61], Attention Transfer (AT) [80], Probabilistic Knowledge Transfer (PKT) [54], and Ensemble (the projector ensemble method of [15]). The cross-task improvement using the inverted projection is most pronounced with FitNets and Ensemble, but some improvement can also be seen on AT and PKT. All teachers produce improvement over the baseline (where no teacher is used and

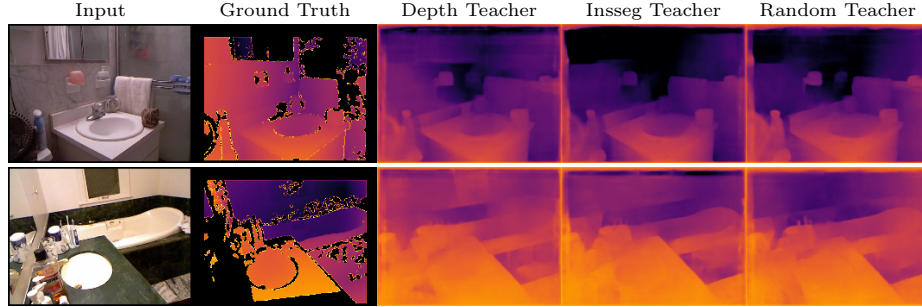


**Fig. 2: Qualitative results on NYUv2 (depth) using different teacher tasks:** results from depth estimation, instance segmentation, and randomly-initialised teachers on a MobileNetV2 [24] student. In each case, we use the optimal projection type for the teacher task: the depth teacher’s task-specific knowledge is desired, so we use a traditional projection, whereas the instance segmentation and random teachers both have irrelevant knowledge that must be discarded and so perform best with our novel inverted projection, which is able to remove the irrelevant features if needed.

the student is trained in isolation) with almost all methods. This indicates that in the case where it is uncertain the degree to which the teacher and student tasks are dissimilar, the use of our inverted projection will in general not be harmful.

We also provide qualitative examples using same-task, similar-task, and randomly-initialised teachers on a different depth estimation student, shown in figure 2. In all cases, we are able to obtain qualitatively good performance.

### 4.3 Semantic segmentation

Semantic segmentation is the task of labelling every pixel in the input image with a class. Our experiments are performed using MSCOCO [41], an 80-class segmentation dataset. We validate the effectiveness of our inverted projector using segmentation, classification, or randomly initialised teachers. In all experiments, we use a simple L2 loss between the projected teacher features and the student features. The results can be seen in table 2a. We are able to obtain significant improvement with all the teacher tasks considered, with the best improvements seen with the random teacher. This follows: both classification and semantic segmentation have significant overlap in knowledge, but the random teacher has significant task-irrelevant information that our inverted projection is able to discard. This further empirically validates the regularisation components described in equation 5.

### 4.4 Image-to-image translation

We experiment with two image-to-image translation tasks: transforming satellite images into maps, and colourisation of black-and-white images. These two student

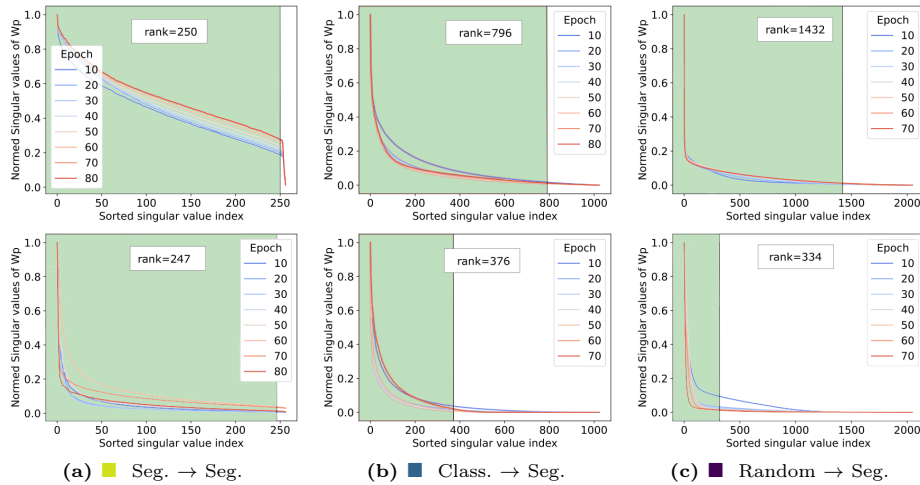


**Fig. 3: Evolution of singular values** of the projection matrix  $\mathbf{P}$  under different cross-task settings and projector types. An L2 loss is used. Green area highlights the rank of  $\mathbf{P}$ . The projection tends towards a higher rank either when using the traditional projection or when using a same-task or similar-task teacher. The low-rank when using our inverted projection in the cross-task setting allows irrelevant features to be filtered out, if necessary for the task pair. **Top row:** traditional projection, **Bottom row:** our inverted projection. Numerical rank is used with a tolerance set to  $\sigma_1 * 0.01$ .

tasks are particularly important, as they do not have significant knowledge overlap with any of the teacher tasks used: classification, depth estimation, instance segmentation, and the randomly-initialised teacher. In contrast, segmentation and classification both share a common goal of understanding the semantic context of the world, while depth estimation and segmentation have been shown to aid one another in the literature (see section 2). The results are shown in tables 2c and 2b. Given the relative dissimilarity of the student tasks with all teacher tasks, it is not surprising that our inverted projection performs well in all cases. We are able to use our inverted projection to produce a significant improvement over the baseline with all teacher tasks, including with the randomly initialised teacher.

#### 4.5 Training Dynamics of the Inverted Projector

By observing the singular value spectrum of the projector weights and how they evolve over the course of training, we are able to provide further insight into the role of our novel inverted projection for cross-task distillation, as compared to the traditional projection. Figure 3 shows the singular value spectrum of the projector weights throughout the training process of a segmentation student with both similar and different teacher tasks, using either the traditional projection or our novel inverted projection. It can be seen that the traditional projection fails to disregard many of the less-dominant singular values, leading to a higher-rank

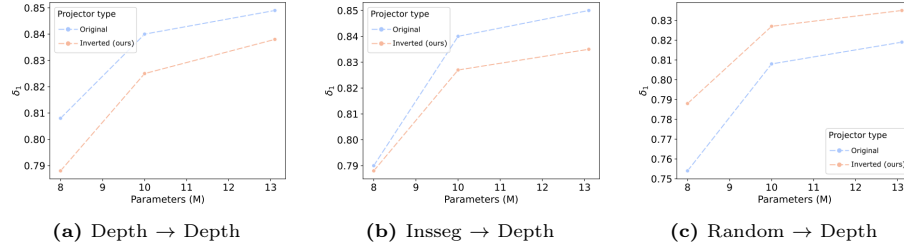


**Fig. 4: Comparing performance of different-sized depth students** with both the traditional projection and our novel inverted projection. Where there is knowledge to transfer from teacher to student (i.e. the two tasks are similar), the traditional projection performs better, but when the teacher is random, the opposite is true. Only decoder size is varied. A MobileNetV2 [24] is used as the backbone.

projection in general. As discussed in section 3.2, this is especially detrimental when there is a significant task gap, as it encourages the student to learn task-irrelevant features. When the student model is small, this can significantly degrade the target task performance. However, when using our inverted projection, we observe a consistently lower rank across training for all tasks, compared to the traditional projection. This is because of the inverted projection’s ability to suppress the task-irrelevant singular vectors from the teacher model: while the traditional projection remains consistently high-rank regardless of the dissimilarity of the student and teacher tasks, our inverted projection is able to adapt to discard the increasing quantity of undesirable task-specific knowledge encoded in the increasingly dissimilar teacher features.

#### 4.6 Ablation Study

**Teacher-free distillation.** As shown in sections 4.2, 4.3, and 4.4, we are able to obtain significant performance improvements even when the teacher is randomly initialised and then frozen, thus containing no task-specific knowledge at all. This reinforces the conclusion reached in section 3.4: the distillation loss function  $\mathcal{L}_{distill}$  may be comprised of a *knowledge transfer* component and a *spectral regularisation component*. In the case where there is no knowledge to transfer between the teacher and the student, only a regularising effect can explain the performance improvement over the baseline.

To control for this, and to provide further evidence of the loss decoupling described in equation 5, we perform experiments using the *spectral regularisation loss* defined in equation 6. We experiment with different values of  $r$  to vary the strength of the loss using a depth estimation student model to be trained on NYUv2 [66] with no teacher model. The results are shown in table 3, and show that our spectral regularisation loss improves performance significantly over the baseline for all values of  $r$  tried, with  $r = 2$  producing the greatest improvement. This finding is significant, as it gives additional support to the decoupling of  $\mathcal{L}_{distill}$  into knowledge transfer and regularisation terms (as shown

**Table 3: Teacher-free distillation** using our spectral regularisation loss on the NYUv2 dataset using AiT [53] on a SwinV2-b base. The regularisation loss is generally robust to different values of  $r$ , with  $r = 2$  being optimal.

Method	RMS ↓	Abs ↓	$\delta_1$ ↑
(Baseline) AiT (SwinV2-B) [53]	0.365	0.105	0.907
$\mathcal{L}_{spectral}$ ( $r = 1$ )	0.352	0.105	0.902
$\mathcal{L}_{spectral}$ ( $r = 2$ )	<b>0.340</b>	<b>0.096</b>	<b>0.914</b>
$\mathcal{L}_{spectral}$ ( $r = 4$ )	0.349	0.099	0.911
$\mathcal{L}_{spectral}$ ( $r = 8$ )	0.344	<b>0.096</b>	0.910
$\mathcal{L}_{spectral}$ ( $r = 16$ )	0.348	0.098	0.912
$\mathcal{L}_{spectral}$ ( $r = 32$ )	0.347	0.100	0.909

**Table 4: Comparing our novel teacher-free spectral regularisation loss** to other state-of-the-art KD methods on ImageNet-1K [16]. Top row is the teacher model used by the KD methods that use a teacher. All methods use a DeiT-Ti [71] student model, with DeiT-Ti $\clubsuit$  describing the distilled variant using distillation tokens.

Network	acc@1	#params
RegNety 160 [57]	82.6	84M
<i>Methods using a pre-trained teacher</i>		
DeiT-Ti $\clubsuit$ [71]	74.5	6M
Co-advise [60]	74.9	6M
DearKD [11]	74.8	6M
USKD [77]	75.0	6M
<i>Methods without any teacher</i>		
DeiT-Ti [71]	72.2	5M
Ours: $\mathcal{L}_{spectral}(r = 8)$	<b>74.5</b>	<b>5M</b>

in equation 5), and further validates the use of the randomly-initialised teacher in our comparisons. Additionally, it provides a useful drop-in tool that can enhance performance with little or no additional cost. Since our proposed regularisation loss is an upper bound on feature distillation, an interesting thought is how it compares to other distillation methods. In table 4 we consider knowledge distillation on the large-scale ImageNet-1K dataset, and we observe that our simple regularisation loss achieves competitive performance with many state-of-the-art knowledge distillation methods.

**Different architecture pairs.** To demonstrate the generality of our proposed inverted projection in various cross-task settings, we perform an ablation across several differently-sized student models with similar and dissimilar task pairs. Figure 4 shows that the performance drop or improvement is consistent for both the very small and moderately large student models, across different task pairs. It also mirrors the findings of our previous experiments in sections 4.2, 4.3, and 4.4, showing that the similarity of the teacher and student tasks matters, and that our novel inverted projection performs best when the two tasks are dissimilar.

**Table 5: Comparisons with different architecture pairs.** All experiments perform cross-task distillation from a classification teacher to a depth estimation student. The inverted projection is effective across various student model sizes and with different KD methods in this cross-task setting.

KD Method	Student Arch (backbone) $\longrightarrow$ Projection type	EfficientNet-B0 (5.3M)			ResNet-50 (25.6M)		
		$\delta_1 \uparrow$	Abs. $\downarrow$	RMS $\downarrow$	$\delta_1 \uparrow$	Abs. $\downarrow$	RMS $\downarrow$
<i>None (baseline)</i>	<i>N/A</i>	0.845	0.127	0.440	0.811	0.144	0.480
AT [80]	Original	0.850	0.125	0.433	0.814	<b>0.143</b>	0.477
	Inverted (ours)	<b>0.853</b>	<b>0.123</b>	<b>0.430</b>	<b>0.816</b>	<b>0.143</b>	<b>0.475</b>
	<i>Improvement</i>	<i>0.35%</i>	<i>1.61%</i>	<i>0.79%</i>	<i>0.26%</i>	<i>0.14%</i>	<i>0.38%</i>
PKT [54]	Original	0.851	0.124	0.432	0.816	0.143	0.473
	Inverted (ours)	<b>0.853</b>	<b>0.123</b>	<b>0.431</b>	<b>0.821</b>	<b>0.141</b>	<b>0.470</b>
	<i>Improvement</i>	<i>0.25%</i>	<i>1.29%</i>	<i>0.30%</i>	<i>0.63%</i>	<i>1.19%</i>	<i>0.70%</i>
FitNets [62]	Original	0.845	0.125	0.439	0.812	0.145	0.480
	Inverted (ours)	<b>0.850</b>	<b>0.124</b>	<b>0.434</b>	<b>0.813</b>	<b>0.142</b>	<b>0.476</b>
	<i>Improvement</i>	<i>0.50%</i>	<i>0.53%</i>	<i>1.34%</i>	<i>0.16%</i>	<i>1.93%</i>	<i>0.77%</i>

Table 5 shows results distilling from a classification teacher to a depth student using two student backbones of significantly-different sizes: an EfficientNet-B0 (5.3M params) and a ResNet-50 (25.6M params). These students are chosen to illustrate both a small and a large capacity gap between the student and teacher models. Three different KD methods are used. Our inverted projector outperforms the traditional projector across all metrics for all three KD methods and both student backbone architectures in this cross-task setting, thus demonstrating the generality of our inverted projector for a variety of practical KD settings.

## 5 Conclusion

In this paper we propose the inverted projector as a simple drop-in component for extending many knowledge distillation (KD) methods into cross-task settings, where the teacher’s task differs from the student’s. This inverted projector is able to suppress the irrelevant task-specific features from the teacher, which greatly improves the efficacy of cross-task distillation. We show consistent and substantial improvements across a number of cross-task pairs using our approach. Most notably, we achieve up to a 7.47% improvement for depth estimation by distilling across a significant task-gap. Through analysis, we provide a concrete interpretation and explanation for our results, leading to a natural decoupling of the objective into a knowledge transfer and a spectral regularisation component, and we extend this to demonstrate a novel drop-in teacher-free loss that achieves some of the benefits of knowledge distillation without the use of a teacher. In this work we have highlighted some of the limitations of KD in the cross-task setting, while also providing a step towards broadening its practical applicability in this new domain.

## References

1. Ahn, J.H., Kim, K., Koh, J., Li, Q.: Federated active learning (f-al): an efficient annotation strategy for federated learning (2022) [2](#)
2. Auty, D., Mikolajczyk, K.: Monocular Depth Estimation Using Cues Inspired by Biological Vision Systems. In: International Conference on Pattern Recognition (ICPR) 2022 [4](#)
3. Bai, Y., Fan, L., Pan, Z., Chen, L.: Monocular Outdoor Semantic Mapping with a Multi-task Network. arXiv pre-print (Jan 2019) [4](#)
4. Baldridge, J., Osborne, M.: Active learning and the total cost of annotation. In: Proceedings of the 2004 Conference on Empirical Methods in Natural Language Processing (2004) [2](#)
5. Bhardwaj, K., Suda, N., Marculescu, R.: Dream distillation: A data-independent model compression framework. ICML Joint Workshop on On-Device Machine Learning and Compact Deep Neural Network Representations (ODML-CDNNR) (2019) [1](#)
6. Bhat, S.F., Alhashim, I., Wonka, P.: AdaBins: Depth Estimation using Adaptive Bins. arXiv:2011.14141 [cs] (Nov 2020), arXiv: 2011.14141 [24](#)
7. Chen, L.C., Papandreou, G., Member, S., Kokkinos, I., Murphy, K., Yuille, A.L.: DeepLab: Semantic Image Segmentation with Deep Convolutional Nets, Atrous Convolution, and Fully Connected CRFs. TPAMI (2017) [24](#)
8. Chen, L.C., Papandreou, G., Schroff, F., Adam, H.: Rethinking Atrous Convolution for Semantic Image Segmentation (Dec 2017), arXiv:1706.05587 [cs] [23](#)
9. Chen, L., Wang, D., Gan, Z., Liu, J., Henao, R., Carin, L.: Wasserstein Contrastive Representation Distillation. CVPR (2020) [1](#), [3](#)
10. Chen, P., Liu, S., Zhao, H., Jia, J.: Distilling Knowledge via Knowledge Review. CVPR (2021) [1](#), [3](#)
11. Chen, X., Cao, Q., Zhong, Y., Zhang, J., Gao, S., Tao, D.: Deardk: Data-efficient early knowledge distillation for vision transformers. CVPR (2022) [1](#), [13](#)
12. Chen, X., Wang, S., Fu, B., Long, M., Wang, J.: Catastrophic forgetting meets negative transfer: Batch spectral shrinkage for safe transfer learning. NeurIPS (2019) [4](#)
13. Chen, X., Wang, S., Long, M., Wang, J.: Transferability vs. discriminability: Batch spectral penalization for adversarial domain adaptation. In: PMLR (2019) [4](#)
14. Chen, Y., Xian, Y., Koepke, A.S., Shan, Y., Akata, Z.: Distilling audio-visual knowledge by compositional contrastive learning. CVPR (2021) [1](#)
15. Chen, Y., Wang, S., Liu, J., Xu, X., de Hoog, F., Huang, Z.: Improved Feature Distillation via Projector Ensemble. NeurIPS (2022) [5](#), [6](#), [9](#), [20](#), [21](#), [22](#), [25](#)
16. Deng, J., Dong, W., Socher, R., Li, L.J., Li, K., Fei-Fei, L.: ImageNet: A Large-Scale Hierarchical Image Database. In: CVPR (2009) [13](#)
17. Deng, Z., Zhang, L., Vodrahalli, K., Kawaguchi, K., Zou, J.: Adversarial Training Helps Transfer Learning via Better Representations. arXiv preprint (6 2021) [4](#)
18. Dosovitskiy, A., Beyer, L., Kolesnikov, A., Weissenborn, D., Zhai, X., Unterthiner, T., Dehghani, M., Minderer, M., Heigold, G., Gelly, S., Uszkoreit, J., Houlsby, N.: An Image is Worth 16x16 Words: Transformers for Image Recognition at Scale. In: ICLR (2021) [9](#)
19. Eigen, D., Puhrsch, C., Fergus, R.: Depth Map Prediction from a Single Image using a Multi-Scale Deep Network. In: NIPS (2014) [24](#)
20. Evci, U., Dumoulin, V., Larochelle, H., Mozer, M.C.: Head2Toe: Utilizing Intermediate Representations for Better Transfer Learning. In: ICML. PMLR (2022) [4](#)



21. Fang, G., Song, J., Wang, X., Shen, C., Wang, X., Song, M.: Contrastive Model Inversion for Data-Free Knowledge Distillation. *IJCAI* (2021) [1](#)
22. Fifty, C., Amid, E., Zhao, Z., Yu, T., Anil, R., Finn, C.: Efficiently identifying task groupings for multi-task learning. *NeurIPS* (2021) [4](#)
23. Fonder, M., Van Droogenbroeck, M.: Mid-air: A multi-modal dataset for extremely low altitude drone flights. In: *Proceedings of the IEEE/CVF conference on computer vision and pattern recognition workshops*. pp. 0–0 (2019) [2](#)
24. Fox, M.H., Kim, K., Ehrenkrantz, D.: MobileNetV2: Inverted Residuals and Linear Bottlenecks. *CVPR* (2018) [10](#), [12](#), [23](#)
25. Gao, R., Saar-Tsechansky, M.: Cost-accuracy aware adaptive labeling for active learning. *AAAI* (2020) [2](#)
26. Goodfellow, I.J., Pouget-Abadie, J., Mirza, M., Xu, B., Warde-Farley, D., Ozair, S., Courville, A., Bengio, Y.: Generative Adversarial Networks. *NeurIPS* (6 2014) [24](#)
27. Greenfeld, D., Shalit, U.: Robust Learning with the Hilbert-Schmidt Independence Criterion. *arXiv preprint* (10 2019) [4](#)
28. He, K., Zhang, X., Ren, S., Sun, J.: ResNet - Deep Residual Learning for Image Recognition. *CVPR* (2015) [23](#)
29. Hinton, G., Vinyals, O., Dean, J.: Distilling the Knowledge in a Neural Network. *NeurIPS* (2015) [1](#), [3](#)
30. Huang, S.J., Chen, J.L., Mu, X., Zhou, Z.H.: Cost-effective active learning from diverse labelers. In: *IJCAI* (2017) [2](#)
31. Huang, T., You, S., Wang, F., Qian, C., Xu, C.: Knowledge distillation from a stronger teacher. *NeurIPS* (2022) [1](#)
32. Isola, P., Zhu, J.Y., Zhou, T., Efros, A.A.: Image-to-Image Translation with Conditional Adversarial Networks (Nov 2018), *arXiv:1611.07004 [cs]* [25](#)
33. James, S., Wohlhart, P., Kalakrishnan, M., Kalashnikov, D., Irpan, A., Ibarz, J., Levine, S., Hadsell, R., Bousmalis, K.: Sim-to-real via sim-to-sim: Data-efficient robotic grasping via randomized-to-canonical adaptation networks. *CVPR* (2019) [2](#)
34. Jiao, J., Cao, Y., Song, Y., Lau, R.: Look Deeper into Depth: Monocular Depth Estimation with Semantic Booster and Attention-Driven Loss. In: *ECCV* (2018) [4](#)
35. Kirillov, A., Mintun, E., Ravi, N., Mao, H., Rolland, C., Gustafson, L., Xiao, T., Whitehead, S., Berg, A.C., Lo, W.Y., Dollár, P., Girshick, R.: Segment anything. *ICCV* (2023) [4](#)
36. Kolbeinsson, B., Mikolajczyk, K.: DDOS: The Drone Depth and Obstacle Segmentation Dataset. *arXiv preprint arXiv:2312.12494* (2023) [2](#)
37. Kolbeinsson, B., Mikolajczyk, K.: UCorr: Wire Detection and Depth Estimation for Autonomous Drones. In: *International Conference on Robotics, Computer Vision and Intelligent Systems - ROBOVIS* (2024) [4](#)
38. Komorowski, P., Baniecki, H., Biecek, P.: Towards evaluating explanations of vision transformers for medical imaging. In: *CVPR Workshops* (June 2023) [2](#)
39. Le, D.H., Vo, T.N., Thoa, N.: Paying more Attention to Snapshots of Iterative Pruning : Improving Model Compression via Ensemble Distillation. *BMVC* (2020) [3](#), [6](#)
40. Li, D., Wu, A., Han, Y., Tian, Q.: Prototype-guided Cross-task Knowledge Distillation for Large-scale Models. *arXiv preprint* (12 2022) [4](#)
41. Lin, T.Y., Maire, M., Belongie, S., Hays, J., Perona, P., Ramanan, D., Dollár, P., Zitnick, C.L.: Microsoft COCO: Common objects in context. *ECCV* (2014) [10](#), [23](#)
42. Liu, Y., Chen, K., Liu, C., Qin, Z., Luo, Z., Wang, J.: Structured Knowledge Distillation for Semantic Segmentation. *CVPR* (2019) [3](#)

43. Liu, Z., Hu, H., Lin, Y., Yao, Z., Xie, Z., Wei, Y., Ning, J., Cao, Y., Zhang, Z., Dong, L., Wei, F., Guo, B.: Swin Transformer V2: Scaling Up Capacity and Resolution. CVPR (2022) [9](#), [23](#)
44. Lopez-Paz, D., Bottou, L., Schölkopf, B., Vapnik, V.: Unifying distillation and privileged information. ICLR (2016) [1](#)
45. Malinin, A., Mlodozienec, B., Gales, M.: Ensemble Distribution Distillation. ICLR (2020) [3](#)
46. McCormac, J., Handa, A., Leutenegger, S., Davison, A.J.: SceneNet RGB-D: Can 5M Synthetic Images Beat Generic ImageNet Pre-training on Indoor Segmentation? In: ICCV (2017) [2](#)
47. Merullo, J., Castricato, L., Eickhoff, C., Pavlick, E.: Linearly Mapping from Image to Text Space. ICLR (2023) [25](#)
48. Miles, R., Elezi, I., Deng, J.:  $V_k$ d: Improving knowledge distillation using orthogonal projections. CVPR (2024) [5](#)
49. Miles, R., Mikolajczyk, K.: Cascaded channel pruning using hierarchical self-distillation. BMVC (2020) [1](#)
50. Miles, R., Mikolajczyk, K.: Understanding the role of the projector in knowledge distillation. AAAI (2024) [5](#), [25](#)
51. Miles, R., Rodriguez, A.L., Mikolajczyk, K.: Information Theoretic Representation Distillation. BMVC (12 2022) [3](#)
52. Miles, R., Yucel, M.K., Manganelli, B., Saa-Garriga, A.: MobileVOS: Real-Time Video Object Segmentation Contrastive Learning meets Knowledge Distillation. CVPR (3 2023) [1](#), [3](#)
53. Ning, J., Li, C., Zhang, Z., Geng, Z., Dai, Q., He, K., Hu, H.: All in Tokens: Unifying Output Space of Visual Tasks via Soft Token (Jan 2023), arXiv:2301.02229 [cs] [9](#), [13](#), [23](#)
54. Passalis, N., Tefas, A.: Learning Deep Representations with Probabilistic Knowledge Transfer. ECCV (2018) [6](#), [9](#), [14](#), [20](#), [21](#), [22](#)
55. Raab, C., Váth, P., Meier, P., Schleif, F.M.: Bridging Adversarial and Statistical Domain Transfer via Spectral Adaptation Networks. In: ACCV 2020. Springer International Publishing (2020) [4](#)
56. Radford, A., Kim, J.W., Hallacy, C., Ramesh, A., Goh, G., Agarwal, S., Sastry, G., Askell, A., Mishkin, P., Clark, J., Krueger, G., Sutskever, I.: Learning transferable visual models from natural language supervision. PMLR (2021) [4](#)
57. Radosavovic, I., Kosaraju, R.P., Girshick, R., He, K., Dollár, P.: Designing Network Design Spaces. CVPR (3 2020) [13](#)
58. Raffel, C., Shazeer, N., Roberts, A., Lee, K., Narang, S., Matena, M., Zhou, Y., Li, W., Liu, P.J.: Exploring the Limits of Transfer Learning with a Unified Text-to-Text Transformer. JMLR (2020) [4](#)
59. Ramamonjisoa, M., Lepetit, V.: SharpNet: Fast and Accurate Recovery of Occluding Contours in Monocular Depth Estimation. arXiv preprint (2019), arXiv:1905.08598v1 [4](#)
60. Ren, S., Gao, Z., Hua, T., Xue, Z., Tian, Y., He, S., Zhao, H.: Co-advise: Cross Inductive Bias Distillation. CVPR (2022) [3](#), [13](#)
61. Romero, A., Ballas, N., Ebrahimi Kahou, S., Chassang, A., Gatta, C., Bengio, Y.: FitNets: Hints For Thin Deep Nets. ICLR (2015) [9](#)
62. Romero, A., Ballas, N., Kahou, S.E., Chassang, A., Gatta, C., Bengio, Y.: FitNets: Hints for Thin Deep Nets. arXiv preprint (Mar 2015), arXiv:1412.6550 [5](#), [6](#), [14](#), [20](#), [21](#), [22](#)
63. Ronneberger, O., Fischer, P., Brox, T.: U-net: Convolutional networks for biomedical image segmentation. MICCAI (2015) [2](#)

64. Sanh, V., Debut, L., Chaumond, J., Wolf, T.: DistilBERT, a distilled version of BERT: smaller, faster, cheaper and lighter. *NeurIPS Workshop on Energy Efficient Machine Learning and Cognitive Computing* (2019) [1](#)
65. Sanh, V., Debut, L., Chaumond, J., Wolf, T.: DistilBERT, a distilled version of BERT: smaller, faster, cheaper and lighter. *NeurIPS Workshop on Energy Efficient Machine Learning and Cognitive Computing* (2019) [3](#)
66. Silberman, N., Hoiem, D., Kohli, P., Fergus, R.: Indoor Segmentation and Support Inference from RGBD Images. In: *ECCV* (2012) [6](#), [9](#), [12](#), [20](#), [25](#)
67. Smith, L.N., Topin, N.: Super-Convergence: Very Fast Training of Neural Networks Using Large Learning Rates (May 2018), [arXiv:1708.07120 \[cs, stat\]](#) [25](#)
68. Sung, Y.L., Cho, J., Bansal, M.: VL-ADAPTER: Parameter-Efficient Transfer Learning for Vision-and-Language Tasks. In: *CVPR* (2022) [4](#)
69. Tan, M., Le, Q.V.: EfficientNet: Rethinking Model Scaling for Convolutional Neural Networks. In: *Proceedings of the 36th International Conference on Machine Learning* (2019), [arXiv:1905.11946](#) [6](#), [23](#)
70. Tian, Y., Krishnan, D., Isola, P.: Contrastive representation distillation. *ICLR* (2019) [1](#), [3](#), [5](#)
71. Touvron, H., Cord, M., Douze, M., Massa, F., Sablayrolles, A., Jégou, H.: Training data-efficient image transformers & distillation through attention. *PMLR* (2021) [13](#)
72. Tyleček, R., Šára, R.: Spatial Pattern Templates for Recognition of Objects with Regular Structure. In: Weickert, J., Hein, M., Schiele, B. (eds.) *Pattern Recognition*. pp. 364–374. *Lecture Notes in Computer Science*, Springer, Berlin, Heidelberg (2013) [25](#)
73. Wang, L., Zhang, J., Wang, O., Lin, Z., Lu, H.: SDC-Depth: Semantic Divide-and-Conquer Network for Monocular Depth Estimation. In: *2020 IEEE/CVF Conference on Computer Vision and Pattern Recognition (CVPR)*. pp. 538–547. IEEE, Seattle, WA, USA (Jun 2020) [4](#)
74. Wang, W., Zhu, D., Wang, X., Hu, Y., Qiu, Y., Wang, C., Hu, Y., Kapoor, A., Scherer, S.: Tartanair: A dataset to push the limits of visual slam. In: *2020 IEEE/RSJ International Conference on Intelligent Robots and Systems (IROS)*. pp. 4909–4916. IEEE (2020) [2](#)
75. Xing, D., Shen, J., Ho, C., Tzes, A.: ROIFormer: Semantic-Aware Region of Interest Transformer for Efficient Self-Supervised Monocular Depth Estimation (Dec 2022), [arXiv:2212.05729 \[cs\]](#) [4](#)
76. Yang, C., Pan, J., Gao, X., Jiang, T., Liu, D., Chen, G.: Cross-Task Knowledge Distillation in Multi-Task Recommendation. *AAAI* (2 2022) [4](#)
77. Yang, Z., Zeng, A., Li, Z., Zhang, T., Yuan, C., Li, Y.: From knowledge distillation to self-knowledge distillation: A unified approach with normalized loss and customized soft labels. *ICCV* (2023) [13](#)
78. Ye, H.J., Lu, S., Zhan, D.C.: Distilling cross-task knowledge via relationship matching. In: *CVPR* (2020) [3](#), [4](#)
79. Yuan, M., Peng, Y.: CKD: Cross-task knowledge distillation for text-to-image synthesis. *IEEE Transactions on Multimedia* **8**, 1955–1968 (2020), conference Name: *IEEE Transactions on Multimedia* [4](#)
80. Zagoruyko, S., Komodakis, N.: Paying more attention to attention: Improving the performance of convolutional neural networks via attention transfer. In: *ICLR* (2019) [6](#), [9](#), [14](#), [20](#), [21](#), [22](#)
81. Zamir, A., Sax, A., Shen, W., Guibas, L., Malik, J., Savarese, S.: Taskonomy: Disentangling Task Transfer Learning. [arXiv:1804.08328 \[cs\]](#) (Apr 2018), [arXiv:1804.08328](#) [4](#)


- 82. Zhao, B., Song, R., Qiu, Y.: Decoupled Knowledge Distillation. CVPR (2022) [3](#)
- 83. Zhou, B., Zhao, H., Puig, X., Fidler, S., Barriuso, A., Torralba, A.: Scene Parsing Through ADE20K Dataset. In: CVPR. p. 9 (2017) [25](#)
- 84. Zhu, J.Y., Park, T., Isola, P., Efros, A.A.: Unpaired Image-to-Image Translation using Cycle-Consistent Adversarial Networks. CVPR (3 2017) [24](#)
- 85. Zhuang, F., Qi, Z., Duan, K., Xi, D., Zhu, Y., Zhu, H., Xiong, H., He, Q.: A Comprehensive Survey on Transfer Learning. arXiv preprint (2020) [4](#)

## 6 Supplementary Material

### 6.1 Full monocular depth estimation results

Table 1 shows only some metrics for monocular depth estimation (MDE) on NYUv2 [66] for the sake of brevity. We include here four additional tables showing the performance on all available metrics of a depth estimation student when distilled to from teachers trained for different tasks. Each table also includes metrics for the baseline, which is a student model trained without any distillation setup of any kind (i.e. only the task loss  $\mathcal{L}_{task}$  is used). Full details of the metrics used are in section 6.4. See section 6.2 for complete architectural details and section 6.3 for loss function details.

**Table 6: Depth teacher  $\rightarrow$  Depth student (no task gap).** As expected, in same-task settings, our inverted projection produces a smaller improvement than the traditional projection. *Improvement* is % change using our inverted projection over using the traditional projection. See section 6.2 for model details. Baseline  $\pm$  figures are variance from 3 runs.

Method	Projection type	 Depth ( <i>Most similar</i> ) $\longrightarrow$ Depth						
		$\delta_1 \uparrow$	$\delta_2 \uparrow$	$\delta_3 \uparrow$	Abs. Rel. $\downarrow$	Sq. Rel. $\downarrow$	RMS $\downarrow$	RMSL $\downarrow$
<i>No teacher (baseline)</i>		0.845 $\pm 0.007$	0.974 $\pm 0.001$	0.995 $\pm 0.000$	0.127 $\pm 0.003$	0.078 $\pm 0.002$	0.440 $\pm 0.005$	0.160 $\pm 0.003$
FitNets [62] <i>ICLR 2015</i>	Traditional	<b>0.868</b>	<b>0.979</b>	<b>0.996</b>	<b>0.117</b>	<b>0.069</b>	<b>0.406</b>	<b>0.148</b>
	Inverted (Ours)	0.849	0.976	0.995	0.124	0.075	0.432	0.157
	<i>Improvement</i>	-2.17%	-0.34%	-0.01%	-6.35%	-9.66%	-6.49%	-5.92%
AT [80] <i>ICLR 2017</i>	Traditional	<b>0.856</b>	0.976	<b>0.995</b>	<b>0.122</b>	<b>0.073</b>	0.426	<b>0.155</b>
	Inverted (Ours)	<b>0.856</b>	<b>0.977</b>	<b>0.995</b>	<b>0.122</b>	<b>0.073</b>	<b>0.425</b>	<b>0.155</b>
	<i>Improvement</i>	-0.11%	0.06%	0.01%	-0.08%	0.82%	0.02%	0.00%
PKT [54] <i>ECCV 2018</i>	Traditional	<b>0.854</b>	<b>0.978</b>	<b>0.996</b>	<b>0.122</b>	<b>0.072</b>	0.429	<b>0.155</b>
	Inverted (Ours)	<b>0.854</b>	0.977	<b>0.996</b>	<b>0.122</b>	0.073	<b>0.427</b>	<b>0.155</b>
	<i>Improvement</i>	0.04%	-0.09%	0.02%	-0.16%	-1.38%	0.42%	0.19%
Ensemble [15] <i>NeurIPS 2022</i>	Traditional	<b>0.861</b>	<b>0.978</b>	<b>0.996</b>	<b>0.119</b>	<b>0.070</b>	<b>0.416</b>	<b>0.151</b>
	Inverted (Ours)	0.849	0.975	<b>0.996</b>	0.124	0.076	0.433	0.157
	<i>Improvement</i>	-1.46%	-0.29%	-0.05%	-4.64%	-7.86%	-4.11%	-4.25%

Each table shows a single teacher/student task pair, and compares four different knowledge distillation methods when using both the traditional projection and our inverted projection, as well as including a percentage *Improvement* showing the difference in performance when using our inverted projection compared to the traditional projection.

**Table 7: Instance segmentation teacher  $\rightarrow$  Depth student (small task gap).** The two tasks are different, but are similar enough that the traditional projection produces greater improvements than our inverted projection does with most methods. *Improvement* is % change using our inverted projection over using the traditional projection. See section 6.2 for model details. Baseline  $\pm$  figures are variance from 3 runs.

Method	Projection type	■ Instance Segmentation → Depth						
		$\delta_1 \uparrow$	$\delta_2 \uparrow$	$\delta_3 \uparrow$	Abs. Rel. $\downarrow$	Sq. Rel. $\downarrow$	RMS $\downarrow$	RMSL $\downarrow$
No teacher (baseline)		0.845 ±0.007	0.974 ±0.001	0.995 ±0.000	0.127 ±0.003	0.078 ±0.002	0.440 ±0.005	0.160 ±0.003
FitNets [62] ICLR 2015	Traditional	0.855	0.977	0.996	0.122	0.073	0.425	0.154
	Inverted (Ours)	0.851	0.975	0.995	0.124	0.075	0.431	0.157
	Improvement	-0.41%	-0.25%	-0.02%	-1.78%	-2.52%	-1.31%	-1.68%
AT [80] ICLR 2017	Traditional	0.852	0.976	0.995	0.123	0.075	0.431	0.156
	Inverted (Ours)	0.855	0.978	0.995	0.121	0.073	0.429	0.155
	Improvement	0.42%	0.16%	0.00%	1.38%	1.74%	0.53%	0.77%
PKT [54] ECCV 2018	Traditional	0.857	0.976	0.995	0.123	0.075	0.427	0.155
	Inverted (Ours)	0.854	0.976	0.995	0.123	0.075	0.429	0.156
	Improvement	-0.34%	0.04%	0.01%	-0.08%	-0.13%	-0.44%	-0.52%
Ensemble [15] NeurIPS 2022	Traditional	0.856	0.977	0.996	0.122	0.072	0.425	0.154
	Inverted (Ours)	0.848	0.975	0.995	0.124	0.076	0.435	0.157
	Improvement	-0.95%	-0.16%	-0.05%	-1.64%	-4.70%	-2.16%	-1.88%

**Table 8: Classification teacher  $\rightarrow$  Depth student (larger task gap).** The two tasks are different enough that the setting becomes more “cross-task” than “same-task”, and our inverted projection begins to outperform the traditional student model in terms of improvement over the baseline. *Improvement* is % change using our inverted projection over using the traditional projection. See section 6.2 for model details. Baseline  $\pm$  figures are variance from 3 runs.

Method	Projection type	■ Classification → Depth						
		$\delta_1 \uparrow$	$\delta_2 \uparrow$	$\delta_3 \uparrow$	Abs. Rel. $\downarrow$	Sq. Rel. $\downarrow$	RMS $\downarrow$	RMSL $\downarrow$
<i>No teacher (baseline)</i>		0.845 ±0.007	0.974 ±0.001	0.995 ±0.000	0.127 ±0.003	0.078 ±0.002	0.440 ±0.005	0.160 ±0.003
FitNets [62] <i>ICLR 2015</i>	Traditional	0.845	0.976	0.996	0.125	0.076	0.439	0.158
	Inverted (Ours)	0.850	0.975	0.995	0.124	0.075	0.434	0.157
	<i>Improvement</i>	0.50%	-0.06%	-0.03%	0.53%	0.44%	1.34%	0.80%
AT [80] <i>ICLR 2017</i>	Traditional	0.850	0.976	0.995	0.125	0.076	0.433	0.157
	Inverted (Ours)	0.853	0.976	0.995	0.123	0.074	0.430	0.156
	<i>Improvement</i>	0.35%	0.08%	0.02%	1.61%	3.03%	0.79%	0.83%
PKT [54] <i>ECCV 2018</i>	Traditional	0.851	0.975	0.996	0.124	0.076	0.432	0.157
	Inverted (Ours)	0.853	0.976	0.995	0.123	0.074	0.431	0.156
	<i>Improvement</i>	0.25%	0.05%	-0.03%	1.29%	2.50%	0.30%	0.64%
Ensemble [15] <i>NeurIPS 2022</i>	Traditional	0.852	0.976	0.995	0.124	0.075	0.431	0.156
	Inverted (Ours)	0.847	0.975	0.995	0.125	0.076	0.437	0.158
	<i>Improvement</i>	-0.63%	-0.12%	0.02%	-0.89%	-1.61%	-1.30%	-1.09%

**Table 9: Randomly-initialised teacher  $\rightarrow$  Depth student (largest task gap).** Our inverted projection produces significant improvement. *Improvement* is % change using our inverted projection over using the traditional projection. See section 6.2 for model details. Baseline  $\pm$  figures are variance from 3 runs.

Method	Projection type	■ Random ( <i>Least similar</i> ) $\longrightarrow$ Depth			Abs. Rel. $\downarrow$	Sq. Rel. $\downarrow$	RMS $\downarrow$	RMSL $\downarrow$
		$\delta_1 \uparrow$	$\delta_2 \uparrow$	$\delta_3 \uparrow$				
<i>No teacher (baseline)</i>		0.845 $\pm 0.007$	0.974 $\pm 0.001$	0.995 $\pm 0.000$	0.127 $\pm 0.003$	0.078 $\pm 0.002$	0.440 $\pm 0.005$	0.160 $\pm 0.003$
FitNets [62] <i>ICLR 2015</i>	Traditional	0.828	0.970	<b>0.995</b>	0.134	0.084	0.455	0.167
	Inverted (Ours)	<b>0.851</b>	<b>0.976</b>	<b>0.995</b>	<b>0.124</b>	<b>0.075</b>	<b>0.431</b>	<b>0.156</b>
	<i>Improvement</i>	2.86%	0.58%	0.08%	7.47%	11.15%	5.20%	6.36%
AT [80] <i>ICLR 2017</i>	Traditional	<b>0.857</b>	<b>0.977</b>	<b>0.996</b>	<b>0.121</b>	<b>0.073</b>	<b>0.428</b>	<b>0.154</b>
	Inverted (Ours)	<b>0.857</b>	0.976	0.995	0.122	0.074	<b>0.428</b>	0.155
	<i>Improvement</i>	0.05%	-0.04%	-0.03%	-0.83%	-1.37%	0.09%	-0.39%
PKT [54] <i>ECCV 2018</i>	Traditional	0.856	0.975	<b>0.995</b>	0.123	0.075	0.429	<b>0.155</b>
	Inverted (Ours)	<b>0.858</b>	<b>0.976</b>	<b>0.995</b>	<b>0.122</b>	<b>0.073</b>	<b>0.426</b>	<b>0.155</b>
	<i>Improvement</i>	0.29%	0.10%	0.00%	1.22%	2.80%	0.84%	0.58%
Ensemble [15] <i>NeurIPS 2022</i>	Traditional	0.835	0.973	0.995	0.128	0.079	0.446	0.162
	Inverted (Ours)	<b>0.849</b>	<b>0.976</b>	<b>0.996</b>	<b>0.124</b>	<b>0.075</b>	<b>0.432</b>	<b>0.157</b>
	<i>Improvement</i>	1.74%	0.26%	0.06%	2.75%	4.96%	3.03%	3.39%

Table 6 shows results using a depth estimation teacher. As the teacher and student tasks are identical and the task-specific features in the teacher are desired for the student model, the traditional projection produces a greater performance improvement than our inverted projection.

Table 7 shows results using an instance segmentation teacher. Instance segmentation produces both semantic labels and instance labels, and the semantic masks and labels are known to be useful for depth estimation (see section 2), so while the teacher and student tasks are different, they are similar to one another. Therefore, we see that the traditional projection still outperforms our inverted projection in most cases, as expected.

Table 8 shows results with a classification teacher. This is a cross-task setup: classification is relatively unrelated to monocular depth estimation. As a result, it can be seen that our inverted projection outperforms the traditional projection.

Table 9 shows results with a randomly-initialised and frozen teacher model. The randomly-initialised teacher does not contain any task-specific knowledge whatsoever, and therefore the task-gap between the teacher and the student model is maximised. As this is the most cross-task setting, our inverted projection performs the best in comparison to the traditional projection, as it is only our inverted projection that is able to successfully discard the confounding features present in the randomly-initialised teacher.

## 6.2 Model details

This section details the different student and teacher architectures used for our experiments.



## Depth estimation

**Teacher models** The teacher models used for depth estimation are:

- **Depth teacher:** SwinV2-B [43] pretrained on NYUv2 as part of the All In Tokens [53] framework.<sup>2</sup>, available from the official AiT repository<sup>3</sup>.
- **Instance segmentation teacher:** SwinV2-B pretrained on COCO [41] as part of the All In Tokens framework.
- **Classification teacher:** ViT-B-16 pretrained on ImageNet-1K, available from the torchvision model hub<sup>4</sup>.

**Student Models** The depth estimation students used have one of three backbones:

- MobilenetV2 [24]: In our experiments, we use a width multiplier of 0.5.
- EfficientNet-B0 [69].
- ResNet-50 [28].

The decoders used are (names in **this font**):

- **Decoder:** Conv1x1, then 6 blocks of (LeakyReLU + Conv3x3 + LeakyReLU + Conv3x3). At the input to each of the 6 blocks, an incoming skip connection from the encoder is bilinearly upsampled to match the feature resolution, then concatenated to the features.
- **Decoder\_d12:** The same as **Decoder**, except the second Conv3x3 in each block is replaced with a depthwise convolution to reduce parameters.
- **ULightDecoder\_skip\_4b:** Conv1x1, then 4 blocks of (LeakyReLU + Conv3x3). As in the other decoders, each block receives features from an incoming skip connection, which are upsampled to match the feature resolution and then concatenated.

## Semantic segmentation

**Teacher models** The teacher models used for semantic segmentation are:

- Segmentation teacher: A DeepLab-V3 [8] with a ResNet-50 backbone, pretrained on a subset of MSCOCO that uses only the 20 categories present in the Pascal VOC dataset. Model and checkpoint loaded from torchvision model hub<sup>4</sup>.
- Classification teacher: ResNet-50 [28] pretrained on ImageNet-1K. Model and checkpoint loaded from torchvision model hub<sup>4</sup>.

<sup>2</sup> [https://msravgcghub.blob.core.windows.net/ait-release/checkpoint/ait\\_depth\\_swinv2b\\_ar.pth](https://msravgcghub.blob.core.windows.net/ait-release/checkpoint/ait_depth_swinv2b_ar.pth)

<sup>3</sup> <https://github.com/SwinTransformer/AiT>

<sup>4</sup> <https://pytorch.org/vision/stable/models.html>

**Student model** The student model used for semantic segmentation was a DeepLabV3 [7] with a ResNet50 backbone that is pretrained on ImageNet-1K. The pretrained weights were sourced from the torchvision model hub<sup>4</sup>.

**Satellite-to-map and Colorization** We use the same teacher models described in section 6.2. For the student models on the satellite-to-map experiments, we use a CycleGAN, while for the colorization experiments we use a Pix2Pix model. This Pix2Pix model follows a standard UNet-like architecture with batch norm layers.

### 6.3 Task losses

In addition to the projection loss  $\mathcal{L}_{distill}$ , each student is trained with a task-specific loss  $\mathcal{L}_{task}$  to supervise its output. The task and projection loss components are weighted equally, as in equation 2.

The depth task loss function used is a variant of the Scale-Invariant Log-Loss (SILog), first proposed by [19] and modified by [6]:

$$\mathcal{L}_{SILog} = 10 \sqrt{\frac{1}{K} \sum_{i=1}^K g_i^2 + \frac{0.15}{K^2} \left( \sum_{i=1}^K g_i \right)^2} \quad (7)$$

where ground-truth and predicted depth values for pixel  $i$  are given as  $d_i^*$  and  $d_i$  respectively,  $g_i = \log(d_i) - \log(d_i^*)$  and  $K$  is the total number of pixels with valid depth values. Semantic segmentation students are trained with a pixelwise cross-entropy loss. For the colourization task we use the vanilla GAN loss [26] in addition to an L1 loss with a weighting of 100.0. For the satellite-to-map translation we use the cyclic consistency loss described in the original CycleGAN paper [84].

### 6.4 Evaluation metrics

**Monocular depth estimation.** We use the metrics defined in [19]:

- Abs relative difference (Abs):  $\frac{1}{T} \sum_{i=1}^T \frac{|d_i - d_i^*|}{d_i^*}$ ,
- Squared relative difference (Sq):  $\frac{1}{T} \sum_{i=1}^T \frac{\|d_i - d_i^*\|^2}{d_i^*}$ ,
- RMSE (RMS):  $\sqrt{\frac{1}{T} \sum_{i=0}^T \|d_i - d_i^*\|^2}$ ,
- Log RMSE (RMSL):  $\sqrt{\frac{1}{T} \sum_{i=0}^T \|\log(d_i) - \log(d_i^*)\|^2}$ ,
- The threshold accuracy  $\delta_n$ : % of  $d_i$  s.t.  $\max(\frac{d_i}{d_i^*}, \frac{d_i^*}{d_i}) = \delta < thr$ , where  $\delta_n$  denotes that  $thr = 1.25^n$  (we use  $n \in \{1, 2, 3\}$ ).  $T$  denotes the total number of valid pixels in the ground truth depth map.  $d_i$  and  $d_i^*$  represent the predicted and ground-truth depth values at pixel  $i$  respectively.

## 6.5 Datasets

For semantic segmentation students, we use the ADE20K Scene Parsing dataset [83], a 150-class subset of the full ADE20K dataset. It contains 20210 training images and 2000 testing images from a variety of indoor and outdoor scenes.

For depth estimation students, the NYUv2 dataset [66] is used, an indoor monocular depth estimation dataset containing 24231 training 654 test examples. Students are trained for 25 epochs.

For image colorization and satellite-to-map translation, we use the CMP Facades [72] and Maps datasets used in Pix2Pix [32], both of which are available from <https://efrosgans.eecs.berkeley.edu/pix2pix/datasets/>. The Maps dataset was scraped from Google Maps by the Pix2Pix authors.

## 6.6 Hyperparameters

**Monocular depth estimation.** Depth estimation students were trained for 25 epochs using the AdamW optimizer with a learning rate of  $2e-4$  and weight decay of 0.05. The OneCycle learning rate scheduler was used [67] with the maximum learning rate set to  $2e-4$ . The batch size was set to 16.

**Semantic segmentation.** Semantic segmentation students were trained for 80 epochs using the AdamW optimizer with a learning rate of  $5e-3$  and weight decay of  $1e-2$ . The OneCycle learning rate scheduler was used, with the maximum learning rate set to  $5e-3$ . The batch size was set to 20.

**Image-to-image translation (satellite-to-map, colorization).** Each model for both of these tasks are trained for 200 epochs using the AdamW optimizer with a learning rate of  $2e-4$ . We keep the initial learning rate for the first 100 epochs and then linearly decay the rate to zero over the next 100 epochs with a batch size of 8.

## 6.7 Linear mapping between task spaces

In performing cross-task distillation, we assume there is an overlap in information in the representation spaces across different tasks, following both the work in the literature and intuition (see section 2). [47] demonstrated the existence of a learnable linear mapping between text and image features. Concurrently, research has shown that linear projections are very effective for knowledge distillation [15, 50]. However, a natural unification of these two settings has not been explored.

We experimentally verify the validity of this assumption with a simple toy scenario, in which a frozen encoder pretrained on instance segmentation is connected via a learnable linear projection to a frozen decoder pretrained for depth estimation. Example qualitative results in figure 5 show that the linearly projected cross-task features can be successfully utilized to generate a coherent output, despite both models being frozen. In fact, by only training the linear projector between these two frozen models, we can attain 0.504 RMSE on NYUv2.

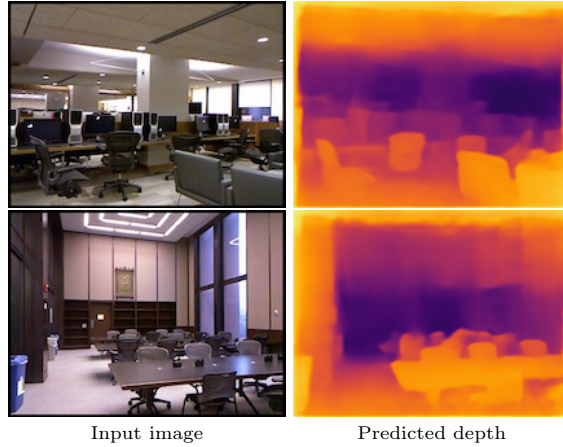


**Fig. 5: Qualitative results using a frozen segmentation encoder and frozen depth decoder.** With only a learned linear projection, features from the semantic segmentation task can be made immediately useful for depth.

This result indicates that a significant portion of the information contained in the instance segmentation features are closely related to the depth estimation task. We conduct additional experiments projecting between various other task representation spaces. These results indicate that cross-task distillation using linear projection is a promising approach for leveraging shared information between specific pairs of tasks, and further motivate our work.

### 6.8 Choice of CycleGAN representation

In the encoder-decoder setup, there is a natural choice for the representation to be used as the distillation loss: the representation at the output of the encoder. However, when dealing with different architectures, the decision is less obvious and can significantly impact the efficacy of the distillation process itself. The CycleGAN architecture consists of a discriminator and two separate encoder-decoder models (generators), which we denote here as  $G_A(\cdot)$  and  $G_B(\cdot)$ . The first of these,  $G_A(\cdot)$ , attempts to generate an image from the input  $\mathbf{x}$  that will fool the discriminator, and the second,  $G_B(\cdot)$ , maps the output of  $G_A(\cdot)$  back to the source domain.

Both  $G_A(\cdot)$  and  $G_B(\cdot)$  are encoder-decoders, and we represent the intermediate features as  $G_{A_E}(\cdot)$  and  $G_{B_E}(\cdot)$  for each respectively. We trialled the use of each set of features, the results of which are shown in table 10, and found a significant improvement when using the representation from the generator that maps back to the source domain:  $\mathbf{Z}_s = G_{B_E}(G_A(\mathbf{x}))$ . Therefore, the features from the second generator  $G_B(\cdot)$  are those used for feature distillation in our main CycleGAN experiments.

**Table 10: Choice of representation** for the distillation loss: either using features from the first generator  $G_A(\cdot)$  that generates the synthetic image, or using features from the second generator  $G_B(\cdot)$  that maps the synthetic image back to the input domain.

Teacher Task	Position	PSNR $\uparrow$	FID $\downarrow$
KeyPoint Det.	$\mathbf{Z}_s = G_{BE}(G_A(x))$	<b>35.77</b>	<b>68.77</b>
KeyPoint Det.	$\mathbf{Z}_s = G_{AE}(x)$	34.97	70.28
Image Classif.	$\mathbf{Z}_s = G_{BE}(G_A(x))$	<b>36.28</b>	<b>59.86</b>
Image Classif.	$\mathbf{Z}_s = G_{AE}(x)$	35.94	66.98

### 6.9 Analysis of Feature Distillation Loss

This section describes the full analysis of the loss function  $\mathcal{L}_{distill}$  detailed in section 3.4 that leads to it breaking into the knowledge transfer component and the regularisation component in equation 5.

### 6.10 Setup and Definitions

We begin by describing our setup. A teacher model,  $T$ , and a student model,  $S$ , both take an identical input to produce the teacher and student features,  $\mathbf{Z}_t \in \mathbb{R}^{b \times d_t}$  and  $\mathbf{Z}_s \in \mathbb{R}^{b \times d_s}$  respectively, where  $d_t$  and  $d_s$  are the sizes of the feature dimensions for the teacher and student models respectively, and  $b$  is the batch size. We also define the inverted projection matrix between the teacher and student feature spaces  $\mathbf{P}$ . The corresponding projected features would be given by  $\bar{\mathbf{Z}}_t = \mathbf{Z}_t \mathbf{P} \in \mathbb{R}^{b \times d_s}$ . The rank  $r$  for each of these is bounded by:

$$r_s = \text{Rank}(\mathbf{Z}_s) \leq \min(b, d_s) \quad (8)$$

$$r_t = \text{Rank}(\mathbf{Z}_t) \leq \min(b, d_t) \quad (9)$$

$$r_p = \text{Rank}(\mathbf{P}) \leq \min(d_t, d_s) \quad (10)$$

$$\bar{r}_t = \text{Rank}(\mathbf{Z}_t \mathbf{P}) \leq \min(r_t, r_p) \quad (11)$$

$$\leq \min(\min(b, d_t), \min(d_t, d_s)), \quad (12)$$

with the latter being due to the fact that  $\text{Rank}(\mathbf{AB}) \leq \min(\text{Rank}(\mathbf{A}), \text{Rank}(\mathbf{B}))$ .

### 6.11 Understanding the Inverted Projection

We demonstrate using our inverted projection. The feature distillation loss function is given by:

$$\mathcal{L}_{distill} = \|\bar{\mathbf{Z}}_t - \mathbf{Z}_s\|_2 = \|\mathbf{Z}_t \mathbf{P} - \mathbf{Z}_s\|_2 \quad (13)$$

Taking the singular value decomposition of each of these gives  $\bar{\mathbf{Z}}_t = \bar{\mathbf{U}} \bar{\Sigma} \bar{\mathbf{V}}^T$  and  $\mathbf{Z}_s = \mathbf{U} \Sigma \mathbf{V}^T$ . Using the rank definitions mentioned previously, we can

express these as sums of products of the singular values and their corresponding singular vectors, i.e.

$$\bar{\mathbf{Z}}_t = \mathbf{Z}_t \mathbf{P} = \sum_{i=1}^{\bar{r}_t} \bar{\sigma}_i \bar{\mathbf{u}}_i \bar{\mathbf{v}}_i \quad (14)$$

$$\mathbf{Z}_s = \sum_{i=1}^{r_s} \sigma_i \mathbf{u}_i \mathbf{v}_i \quad (15)$$

where  $\bar{\boldsymbol{\sigma}} \in \mathbb{R}^{\bar{r}_t}$  and  $\boldsymbol{\sigma} \in \mathbb{R}^{r_s}$  denote the columns of  $\bar{\boldsymbol{\Sigma}}$  and  $\boldsymbol{\Sigma}$  respectively,  $\bar{\mathbf{u}} \in \mathbb{R}^{b \times \bar{r}_t}$  and  $\mathbf{u} \in \mathbb{R}^{b \times r_s}$  the columns of  $\bar{\mathbf{U}}$  and  $\mathbf{U}$ , and  $\bar{\mathbf{v}} \in \mathbb{R}^{\bar{r}_t \times d_s}$ , and  $\mathbf{v} \in \mathbb{R}^{r_s \times d_s}$  the columns of  $\bar{\mathbf{V}}$  and  $\mathbf{V}$ . The feature distillation loss can be rewritten as:

$$\mathcal{L}_{\text{distill}} = \|\bar{\mathbf{Z}}_t - \mathbf{Z}_s\|_2 \quad (16)$$

$$= \underbrace{\left\| \sum_{i=1}^{\bar{r}_t} \bar{\sigma}_i \bar{\mathbf{u}}_i \bar{\mathbf{v}}_i - \sum_{i=1}^{r_s} \sigma_i \mathbf{u}_i \mathbf{v}_i \right\|_2}_{\text{knowledge transfer only}} \quad 1. \text{ Same-task} \quad (17)$$

The rank of the inverted projection matrix dictates how the upper bound on the loss can be decomposed into a knowledge transfer component and a regularisation component. We empirically find that  $\mathbf{P}$  works out to be lower-rank in the cross-task setting (see section 4.5), and so  $r_s > \bar{r}_t$ . This observation allows us to merge the sum in equation 17 such that every one of the  $\bar{r}_t$  projected teacher singular values is compared to a student singular value, with the remaining  $r_s - \bar{r}_t$  student singular values forming the regularisation term:

$$\begin{aligned} \mathcal{L}_{\text{distill}} &= \left\| \sum_{i=1}^{\bar{r}_t} (\bar{\sigma}_i \bar{\mathbf{u}}_i \bar{\mathbf{v}}_i^T - \sigma_i \mathbf{u}_i \mathbf{v}_i^T) + \sum_{i=\bar{r}_t+1}^{r_s} \sigma_i \mathbf{u}_i \mathbf{v}_i^T \right\|_2 \\ &\leq \underbrace{\left\| \sum_{i=1}^{\bar{r}_t} \bar{\sigma}_i \bar{\mathbf{u}}_i \bar{\mathbf{v}}_i^T - \sigma_i \mathbf{u}_i \mathbf{v}_i^T \right\|_2}_{\text{knowledge transfer}} + \underbrace{\left\| \sum_{i=\bar{r}_t+1}^{r_s} \sigma_i \mathbf{u}_i \mathbf{v}_i^T \right\|_2}_{\text{student regularisation}} \quad 2. \text{ Cross-task} \end{aligned} \quad (18)$$

This shows that, under the cross-task setting, the feature distillation contains both a knowledge transfer component (which incorporates information from the teacher model) and a regularisation component (which acts upon the student model).